Journal of Alloys and Compounds 504S (2010) S48–S51

Contents lists available at ScienceDirect

Journal of Alloys and Compounds

journal homepage: www.elsevier.com/locate/jallcom

Relationship between thermophysical and mechanical properties of metallic glasses

Livio Battezzati*, Ahsan Habib, Daniele Baldissin, Paola Rizzi

Dipartimento di Chimica IFM e Centro NIS, Università di Torino, Via P. Giuria 7, 10125 Torino, Italy

ARTICLE INFO

Article history:
Received 3 July 2009
Received in revised form 1 April 2010
Accepted 8 April 2010
Available online 10 May 2010

Keywords:
Metallic glasses
Glass transition
Mechanical properties
Shear band

ABSTRACT

Mechanical (elastic moduli, yield strength, hardness) and thermophysical (glass transition, fragility indexes, heat content of shear bands) properties of metallic glasses are discussed and compared using an extensive database containing values for different families of alloys.

The relationships between some of the above quantities are analysed to get insight into the shear band energetics and propagation. The failure by shear and the consequent temperature rise due to the release of elastic energy are analysed also with the help of a finite element simulation with attention to the length scales for each process. The data for different families of alloys are compared. The results of analyses and simulation are employed for discussing serrated flow and shear band propagation with an example on an Al-based metallic glass.

1. Introduction

The interest on mechanical properties of metallic glasses is increased steadily during the last years when bulk materials have become widely available for both appropriate testing and perspective application [1–3]. The availability of a large number of data obtained with alloys of very diverse formulation has prompted the analysis of correlations among properties, especially thermal and mechanical [4–7]. This activity has two objectives: relating the properties to structural models of the materials also as a function of temperature and attempt predictions of property values not yet available. In this paper such analysis is confined to bulk metallic glasses, but extended to the most recent data appeared in the literature. At first the correlation of strength and moduli with the glass transition temperature, T_g, is revisited taking care of properly subdividing the alloys in their respective families. Then, the energetics of events leading to failure are considered, i.e., local temperature rise after a shear offset and maturation of a catastrophic shear band, again in relationship with the alloy composition, ending with a some notes on serrated flow.

2. Mechanical and thermal properties

It is well established that mechanical properties of metallic glasses correlate with T_g [7]. Examples are reported in Figs. 1 and 2 for the Young's modulus, E, and the yield or fracture strength, $\sigma_{y,r}$, respectively, showing the link between thermal and mechanical variables of metallic glasses. The modulus clearly scales with T_g, although with scatter (Fig. 1). It also must correlate with the melting point, T_m, which scales with the cohesive energy of the solid since the ratio T_g/T_m is often taken as an index of glass forming ability of the alloy being comprised approximately between 0.55 and 0.66 for bulk metallic glasses [1,2]. In addition to the intrinsic properties of the elements, part of the scatter in the E plot can actually be related to the varied proportionality between T_g and T_m. An example is provided by the Fe-based glasses of high modulus and low T_g in relative terms. The data for strength are reported together for tension and compression experiments since they overlap within the respective accuracy [8]. Again, the correlation showing the increase of strength with T_g is apparent (Fig. 2), as well as the deviation from it for Fe-based and some Ni-based glasses. Since the strength of metallic glasses often approaches the theoretical limit for solids, the upper left part of the diagram does not contain points. The trends in Figs. 1 and 2 are qualitatively similar reflecting the well known fact that the elastic deformation at yielding, i.e., the ratio of $\sigma_{y,r}$ to E, is of the order of 2% [3].

The set of data collected here for bulk metallic glasses refer to tensile/compressive experiments performed at room temperature. Deformation of metallic glasses is homogeneous close to the glass transition temperature, T_g, and inhomogeneous at low temperature occurring in localized shear bands which are triggered by the activation of a shear transformation zone [3]. It has been argued that a critical strain level is necessary for the occurrence of such event and that the critical strain should decrease on increasing temperature towards the glass transition because of thermal activation of cooperative shear [4]. The tensile/compressive strain is plotted

* Corresponding author.
E-mail address: livio.battezzati@unito.it (L. Battezzati).

0925-8388/$ – see front matter © 2010 Elsevier B.V. All rights reserved.
doi:10.1016/j.jallcom.2010.04.034

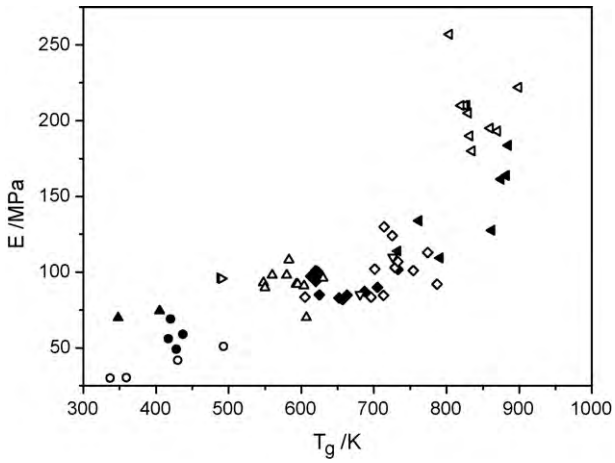

Fig. 1. The correlation between Young's modulus and T_g for bulk metallic glasses. *Symbols*: (▲) Au-based, (■) Ca-based, (◊) Cu-based, (◁) Fe-based, (●) Mg-based, (◀) Ni-based, (△) Pd-based, (▷) Pt-based, (○) rare earth-based, (▽) Ti-based, (⧫) Zr-based.

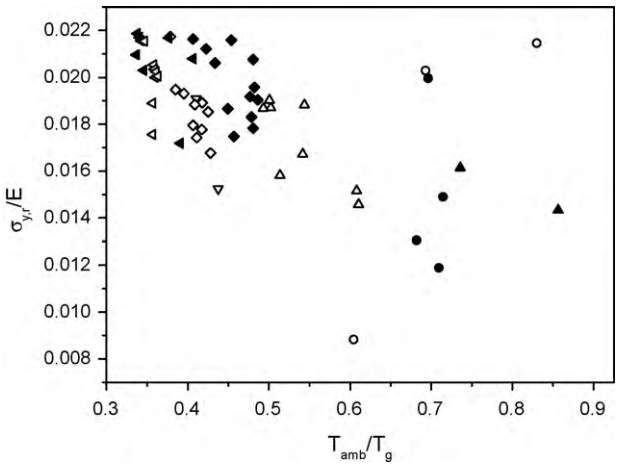

Fig. 3. The tensile/compressive strain plotted versus the measurement temperature scaled with respect to T_g for bulk metallic glasses. Symbols as in Fig. 1.

versus the measurement temperature scaled with respect to T_g in Fig. 3. The decrease of the strain with temperature is confirmed for most families of glasses. Since metallic glasses are believed to yield via the Mohr–Coulomb criterion, the shear and normal stresses are related via a friction coefficient [3]. The use of data as in Fig. 3 implies assuming a constant pressure dependence of the shear stress, i.e., friction coefficient, for all glasses. Deviation from the approximation of a constant value might explain some of the differences between glass types.

3. Elastic properties of the glass and thermophysical properties of the liquid

The recent literature has reported a debate on the possibility that the elastic properties of the glass could embed some information on structure sensitive quantities of its liquid state [5,9–11]. This stems from the observation that the local structure of the liquid is frozen-in upon vitrification. The quantity upon which attention was drawn is the liquid fragility as expressed either by the slope of the liquid viscosity or by that of entropy loss on approaching T_g [12]. The fragility was suggested to scale linearly with both the Poisson ratio, ν, and the ratio of bulk to shear moduli, B/G [9]. The evidence collected to date shows that the fragility of metallic glasses depends weakly on T_g [13]. Fig. 4 shows that the B/G ratio scales with T_g only roughly. These representations, therefore, provide a hint on the possible correlation between liquid and glass properties, but also the indication that they cannot be used for prediction since may differ for each group of material.

Egami has developed a model of amplitude fluctuations in the liquid based on uncorrelated atomic level stresses. When the liquid becomes a glass, the local stress causes a long-range elastic field-inducing freezing of topology. The model links the related total elastic energy to the thermal energy to be supplied to the material to unrelax it at the glass transition [14]. The relevant equation is

$$\frac{RT_g}{4} = \frac{BV}{2K_\alpha}\left\langle \left(\varepsilon_V^{\mathrm{crit}}\right)^2 \right\rangle \quad (1)$$

where V is the molar volume, R the gas constant, $\left\langle \left(\varepsilon_V^{crit}\right)^2 \right\rangle$ the ensemble average of the volume strain and K_α is the following function of the Poisson ratio

$$K_\alpha = \frac{3(1-\nu)}{2(1-2\nu)} \quad (2)$$

Fig. 5 reports a plot of B versus the volumetric thermal energy corrected for the K_α term. Although the correlation in Fig. 5 cannot be considered as predictive for an unknown property of the mate-

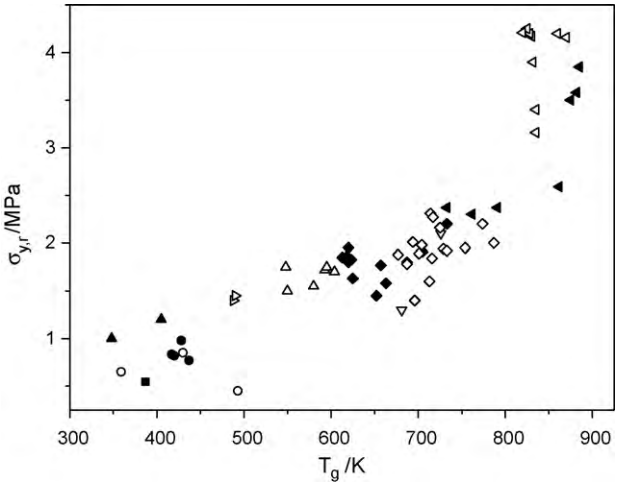

Fig. 2. The correlation between yield/fracture stress and T_g for bulk metallic glasses. Symbols as in Fig. 1.

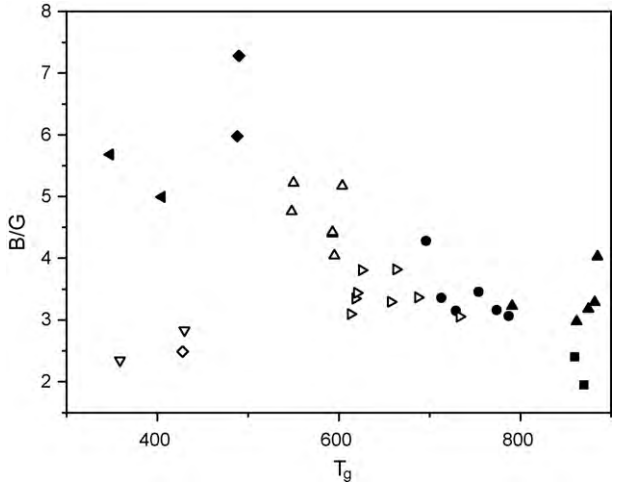

Fig. 4. The bulk to shear modulus ratio versus T_g for bulk metallic glasses. Symbols as in Fig. 1.

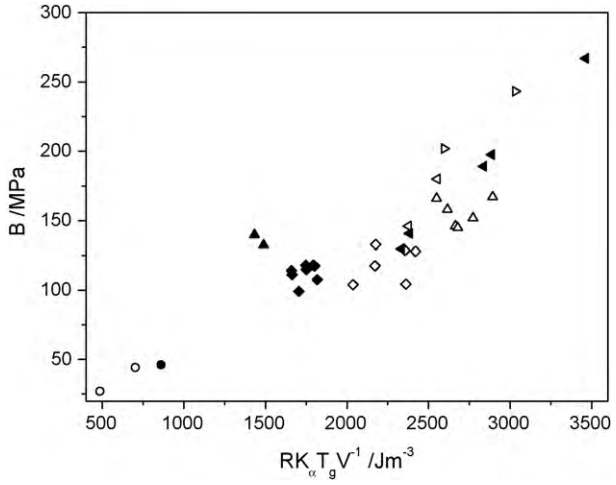

Fig. 5. The Egami plot expressed by Eq. (1) for bulk metallic glasses. Symbols as in Fig. 1.

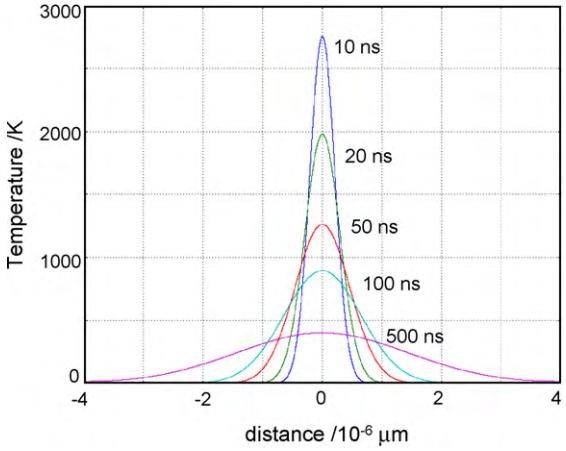

Fig. 7. Temperature profiles of heat evolution in a shear band from FE modelling as a function of distance in the material for various times for a $Fe_{57.6}Co_{14.4}B_{19.2}Si_{4.8}Nb_4$. The curves show the temperature rise with respect to the testing temperature, taken as room temperature.

rial, it represents, however, the best one reported to date between elastic and thermophysical properties of metallic glasses.

4. Length scales of temperature profiles around shear bands

The correlation of $\sigma_{y,r}$ to T_g shown above suggests investigating the possible role of the glass transition in the failure of metallic glasses. Shear displacement occurs at some flaw of the material. Then, the critical shear band becomes operative propagating with loss of traction. Elastic energy is contributed to the band and the temperature rises [3]. Determination of the heat content of shear bands based on the fusible coating method and calculations of the corresponding temperature rise using data for Vitreloy 1 (Vit 1, $Zr_{41.25}Ti_{13.75}Ni_{10}Cu_{12.5}Be_{22.5}$) [15,16] showed that T_g can be definitely exceeded. Starting from these data, it has been argued [13,17] that the energy released at fracture is expressed by the resilience of the metallic glass ($U_r = \sigma_{y,r}^2/2E$). The thermal energy needed to bring the glass to T_g is approximately $U_t = 3R\Delta T_g/V$ with ΔT_g the difference between T_g and the testing temperature [6,17]. U_r shows a clear correlation versus U_t as reported in Fig. 6 for bulk metallic glasses. Most points fall in the lower part of the diagram and the upper triangle is empty since the theoretical strength cannot be exceeded. As already noted for ribbons [13], for each value of thermal energy there is scatter of data, even for the same alloy. The likely source of this scatter is the uncertainty in the yield stress of materials of different shape and size prematurely fractured during testing.

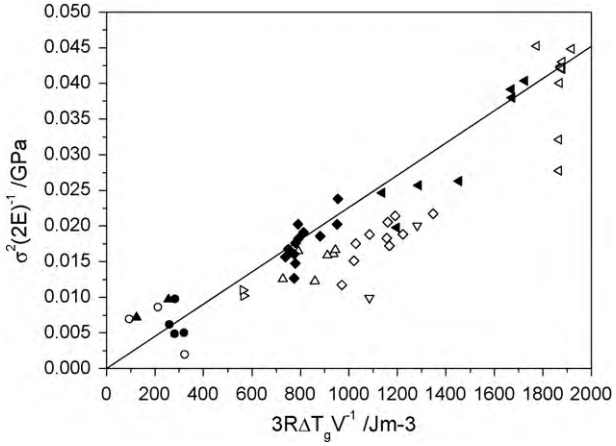

Fig. 6. The resilience of bulk metallic glasses versus the volumetric amount of heat needed to bring the material from room to the glass transition temperature. The line is defined in the text. Symbols as in Fig. 1.

The above events occur on three length scales: the first one corresponds to the thickness of the volume of unit area defining the shear band, i.e., a few tens of nanometers, a second one corresponding to the volume of unit area providing mechanical energy estimated as tens to hundreds of micrometres thick, and a third one related to the volume of unit area where localization of elastic energy occurs resulting of the order of a few micrometers where temperatures in excess of T_g are experienced [17]. The extent of this zone is compatible with the size of the molten zones in fusible coating experiments [16] and of veins and other features on the fracture surfaces of metallic glasses [18]. From the above calculation for Vit1, U_t results 44 times U_r implying that excess energy is localized in the band and then dissipated by conduction. In Fig. 6 a straight line joining the origin to the Vit 1 point is drawn. It appears to correspond approximately to the limit for the accessible part of the diagram for several families of bulk metallic glasses (Zr-, Mg-, Pd-, Ni- and Fe-based) indicating that shear band propagation is related to T_g for many alloys in the same way. It is noted that at least the points for Cu-based alloys deviate from the stated correlation, although aligned on a roughly parallel line, showing that assumptions made in calculations may not be all generally applicable.

The temperature profile around the shear band was computed by means of Finite Element modelling assuming the heat source is a thin slab of the same width as shear bands, taken here as 10 nm [19], adjacent to a thicker domain, the heat reservoir, where heat conduction occurs [17]. An example of the resulting temperature profiles is given in Fig. 7 for a Fe-based glass chosen because its U_t to U_r values lie on the straight line in Fig. 6. Spatial temperature profiles at various times after shearing are reported. The temperature decreases rapidly in time and space but a region of some hundred nanometers thickness remains above T_g still after 5×10^{-8} s. These times are of the same order as that estimated for shearing, therefore the band is not adiabatic, as already pointed out [16,17,19]. The temperature is still above the glass transition (about 830 K) close to 500 ns. The cooling rate from the melting point to T_g is of the order of 10^9 K/s well suited to keep the zone glassy after shearing, however, the relatively long permanence of the band at high temperature can contribute to the brittleness of the glass.

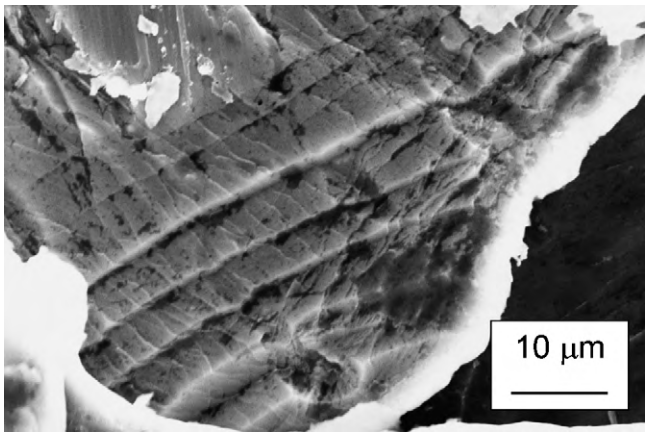

Fig. 8. Steps on the surface of a fragment of an $Al_{87}Ni_7Ce_6$ ribbon heavily cold rolled to fracture while embedded in an Al envelope serrated between stainless steel plates.

5. Serrations

The shear band energetics discussed above refers to catastrophic failure. Bulk metallic glasses often present plastic behaviour via a series of serrations. Each of them implies stress drops of the order of 1% and elastic deformation with energy release of the order of $10^{-4} \times U_r$ per serration [20,21]. As for de-cohesion in stick-slip processes [22], this implies that the amount of energy released refers to a limited volume of matter; using the figure derived above and taking a unit area across the material, it is estimated it extends from submicron to a few microns distances. Under compression this does not cause initiation of a crack. Dissipation of heat takes place fast and the stress can rise again until a new serration occurs of increased extent. This process continues until a critical serration size or a runaway crack develops leading to fracture. As a consequence of serrated flow the movement of related shear bands produces steps of various sizes on the surface of samples [16,20]. In these cases, temperature rises should be more limited than for fracture, and T_g, may not be reached. Actually, it is reported that the size of the molten zone in fusible coating experiments scales with the shear offset of each band becoming undetectable below about 1 μm [16]. The steps produced on the material surface display the presence of molten matter in some cases [20] but, at variance, often they have sharp edges. An example is provided in Fig. 8 where a large number of steps are seen on the surface of a fragment of an $Al_{87}Ni_7Ce_6$ ribbon cold rolled to fracture being embedded in an Al envelope serrated between stainless steel plates. Steps of various orientation are apparent due to mixed mode deformation. No sign of melting can be detected even for steps of several micron size. In the same sample, however, molten features were found on some external surfaces of fragments possibly broken in tension [21]. The present analysis suggests a qualitative interpretation of such microstructural features, but detailed modelling of heat dissipation as a consequence of local plasticity is needed for demonstration.

Acknowledgments

Work performed for "Progetto D23, Bando Regionale Ricerca Scientifica Applicata 2004". Fondazione S. Paolo is acknowledged for support to CdE NIS.

References

[1] A.L. Greer, Mater. Today 12 (2009) 14–22.
[2] A.L. Greer, E. Ma (Eds.), MRS Bull. 32 (2007) 611–615 (and ff).
[3] C.A. Schuh, T.C. Hufnagel, U. Ramamurty, Acta Mater. 55 (2007) 4067.
[4] W.L. Johnson, K. Samwer, Phys. Rev. Lett. 95 (2005) 195501.
[5] L. Battezzati, Mater. Trans. 46 (2005) 2915–2919.
[6] B. Yang, C.T. Liu, T.G. Nieh, Appl. Phys. Lett. 88 (2006) 221911.
[7] W.H. Wang, J. Appl. Phys. 99 (2006) 093506.
[8] L. Battezzati, D. Baldissin, M. Baricco, T.A. Baser, D. Firrao, P. Matteis, G.M.M. Mortarino, Mater. Res. Soc. Sympos. Proc. 1048 (2008), 1048-Z02-08.
[9] V.N. Novikov, A.P. Sokolov, Nature 431 (2004) 961–963.
[10] S.N. Yannopoulos, G.P. Johari, Nature 444 (7118) (2006) E8.
[11] V.N. Novikov, A.P. Sokolov, A. Kisliuk, Philos. Mag. 87 (2007) 613–621.
[12] L. Battezzati, A. Castellero, P. Rizzi, J. Non-Cryst. Solids 353 (2007) 3318–3326.
[13] L. Battezzati, G.M.M. Mortarino, J. Alloys Compd., 10.1016/j.jallcom. 2008.08. 099.
[14] T. Egami, J. Alloys Compd. 434–435 (2007) 110–114.
[15] J.J. Lewandowski, A.L. Greer, Nat. Mater. 5 (2006) 15.
[16] Y. Zhang, L.A. Stelmashenko, Z.H. Barber, W.H. Wang, J.J. Lewandowski, A.L. Greer, J. Mater. Res. 22 (2007) 419.
[17] L. Battezzati, D. Baldissin, Scripta Mater. 59 (2008) 223–226.
[18] P. Rizzi, L. Battezzati, J. Non-Cryst. Solids 344 (2004) 94.
[19] Y. Zhang, A.L. Greer, Appl. Phys. Lett. 89 (2006) 071907.
[20] K. Georgarakis, M. Aljerf, Y. Li, A. LeMoulec, F. Charlot, A.R. Yavari, K. Chornokhvostenko, E. Tabachnikova, G.A. Evangelakis, D.B. Miracle, A.L. Greer, T. Zhang, Appl. Phys. Lett. 93 (2008) 031907.
[21] L. Battezzati, D. Baldissin, A. Habib, P. Rizzi, J. Phys.: Conf. Ser. 144 (2009) 012088.
[22] F. Brochard-Wyart, P.-G. deGennes, Eur. Phys. J. E 23 (2007) 439–444.